Korean J. Chem. Eng., **16**(2), 265-273 (1999)

EXPERIMENTAL ELECTROHYDRODYNAMICS OF POLY(γ-BENZYL-L-GLUTAMATE) IN M-CRESOL SOLUTION SUBJECTED TO SHEAR FLOW AND ELECTRIC FIELDS

Moo Hyun Kwon, Young Sil Lee and O Ok Park†

Department of Chemical Engineering, Korea Advanced Institute of Science and Technology,
373-1, Kusung-dong, Yusong-gu, Taejon 305-701, Korea
(Received 30 October 1998 • accepted 10 February 1999)

Abstract–Electrohydrodynamics of a dilute solution of rigid macromolecules was experimentally studied in a continuation of previous theoretical work. We used poly(γ-benzyl-L-glutamate), having 4 different molecular weights ranging from 15,000 to 236,000, dissolved in m-cresol. Poly(γ-benzyl-L-glutamate) solutions were subjected to combinations of simple shear flow field and uniform electric field perpendicular to the shear direction. Transient birefringence and extinction angle were simultaneously measured using the phase-modulated birefringence method. Steady state results were compared with the theoretical prediction from previous works and rotational diffusivity and permanent dipole strength of PBLG were obtained from multiple parameter fitting. Consequently, the optical state of PBLG solution could be explained to a certain extent by the dimensionless field parameters established in the previous theory.

Key words : Electrohydrodynamics, Poly(γ-benzyl-L-glutamate), Birefringence, Extinction Angle, Phase-Modulated Birefringence Method

INTRODUCTION

For the characterization and processing of functional polymers, it is necessary to understand not only their rheological properties but also electro-optical properties. Research interests up to now have been usually restricted to one aspect of them. In the past, birefringence experiments by a single external field such as hydrodynamic, electric or magnetic field have been studied separately, each with its own research purpose [Arp et al., 1980; O'Konski, 1976]. Electric birefringence of polymer solutions has been used as one of the characterization tools, and rheological measurements have been usually done for the processing purpose.

In the present work, as an experimental part of the previous theoretical works [Park, 1988, 1989; Kwon and Park, 1992], the effects of the combined (shear and electric) fields on the rigid macromolecules dissolved at low concentration in a dielectric Newtonian solvent were investigated using optical functions such as birefringence and extinction angle. In the previous work, the model solution of a rigid Brownian polymer with dipoles was presented and analyzed in terms of the dimensionless field parameters. A better insight into both microscopic properties of macromolecules and macroscopic properties in relation to its molecular properties could be obtained. Depending on the types of external fields or the object solution being considered, an experimental method or analysis of the results should be selected properly.

Flow birefringence experiments have generally been performed from a rheological aspect, related to the hydrodynamic characteristics of dissolved particles [Meeten, 1986; O'Konski, 1976]. Electric (or magnetic) birefringence experiments have mainly focused on investigating the electric (or magnetic) and optical properties [O'Konski et al., 1959]. Characteristics of a polymer solution can be appreciated in detail by a transient birefringence experiment under the combined field [Ikeda, 1963; Mukohata et al., 1962].

Transient birefringence experiments were performed here under simultaneous hydrodynamic and electric fields using several m-cresol solutions of poly(γ-benzyl-L-glutamate), PBLG, with different molecular weights. Some experimental results with various combinations of the external fields were compared with the theoretical prediction from the previous work [Kwon and Park, 1992]. In order to interpret the experimental birefringence results under the combined fields, the following dimensionless groups are defined [Park, 1988; Kwon and Park, 1992];

$$\alpha=\frac{G}{D_r}; \qquad D_r=\frac{3kT}{4\pi a^3\mu_0}r^2Q(r), \tag{1}$$

$$\beta=\frac{VB_a\mu_0E_0}{kT} \tag{2}$$

Here α, Peclet number, is the dimensionless flow strength compared with Brownian force of a polymer, β, related to the permanent dipole moment of a polymer. G is the shear rate, D_r the rotational diffusivity of a polymer, k the Boltzmann constant, T the absolute temperature, η_0 the viscosity of Newtonian solvent, V the volume of a particle, B_a the internal field function [O'Konski, 1976], μ_0 the permanent dipole moment per unit volume of a polymer particle. $VB_a\mu_0$ is the permanent dipole strength of a particle, E_0 the electric field strength, and r (=a/b) the aspect ratio

†To whom correspondence should be addressed.
E-mail : oopark@sorak.kaist.ac.kr

where 2a and 2b are the length of major and minor axes, respectively. And the geometric factor $r^2Q(r)$ can be approximated as

$$r^2Q(r)=\frac{\ln(2r)-0.5}{2}, \quad r>2. \tag{3}$$

It is generally accepted that PBLG molecule has negligible induced dipole moment even in a very high saturating electric field [O'Konski et al., 1959]. Therefore only the permanent dipole moment is considered in this study.

The rotational diffusivity D_r of PBLG molecule can be estimated by using Eq. (1). It is generally reported that the typical length of the repeating unit of PBLG is approximately 0.15 nm. A molecular weight of 236,000 corresponds to 2a length of 1.62×10^{-7} m [Mukohata et al., 1962]. With 2b equal to 1.60×10^{-9} m, D_r is estimated to be 217 sec^{-1}. Mukohata et al. [1962] reported that D_r of PBLG with the weight average molecular weight of 206,000 was estimated to be 220 sec^{-1} from the initial slope of cot 2χ vs. shear rate in their birefringence experiment in the weak fields. They also obtained the residual permanent dipole strength of PBLG as 3.4 Debye unit. The value of the residual permanent dipole moment agrees satisfactorily with that of peptide bond. Similar results can be found elsewhere, i.e., estimated from the saturating electric birefringence [O'Konski et al., 1959] and from dielectric dispersion [Wada, 1959].

EXPERIMENTAL

1. Phase-Modulated Flow Birefringence (PMFB)

The rheo-optical state of a solution changes according to the solute behavior by the external fields. Optical measurements as non-destructive methods to trace such changes have been steadily advanced during the last decades. The phase-modulated flow birefringence method, PMFB [Frattini and Fuller, 1984; Oh and Park, 1992], which was adopted in our experiments, allows us to make simultaneous measurement of both transient birefringence and extinction angle. It was successfully applied for polystyrene solution to measure the rheological properties [Hwang et al., 1989].

The basic principle of this technique is to extract the first and second harmonics due to the reference frequency ω of the photo-elastic modulator, PEM, to give a sinusoidal modulation to the source light. Fig. 1 is the schematic representation of the PMFB apparatus used in this study. The orientations of the external fields and other optical elements used are shown in Fig. 2. The polarized He-Ne laser light is transmitted through several optical elements and the streaming Kerr cell containing the solution, and is detected at the photo-diode detector. Birefringence and extinction angle evoked by the external fields can be effectively obtained by the Muller matrix calculation scheme. If the incident light is presented as Stokes vector $\mathbf{S}_0$, the Stokes vector $\mathbf{S}$ for the light leaving the optical arrangements can be expressed as follows:

$$\mathbf{S}=\mathbf{M}_p(-45°)\mathbf{M}_q(0°)\mathbf{M}_s(\phi)\mathbf{M}_q(0°)\mathbf{M}_m(45°)\mathbf{M}_p(90°)\mathbf{S}_0 \tag{4}$$

where $\mathbf{M}_i$ is the Muller matrix of each optical component i, details of which are given in the reference of Shurcliff [1962].

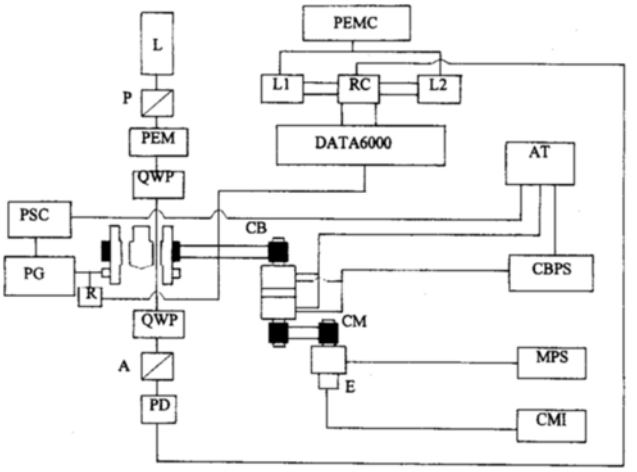

Fig. 1. Schematic diagram of phase-modulated flow birefringence system with electric field unit.

A : Analyzer	L2 : 2ω lock-in amplifier
AT : Main computer	MPS : CM power supply
CB : Clutch/Brake	P : Polarizer
CBPS : CB power supply	PD : Photo-decector
CM : Compumotor	PEM : Photo-elastic modulator
CMI : CM index	PEMC : PEM controller
D6 : DATA 6000	PG : Pulse generator
E : Encoder	PSC : PG controller
L : Laser	R : Resister connection
L1 : ω lock-in amplifier	RC : Ratio circuit

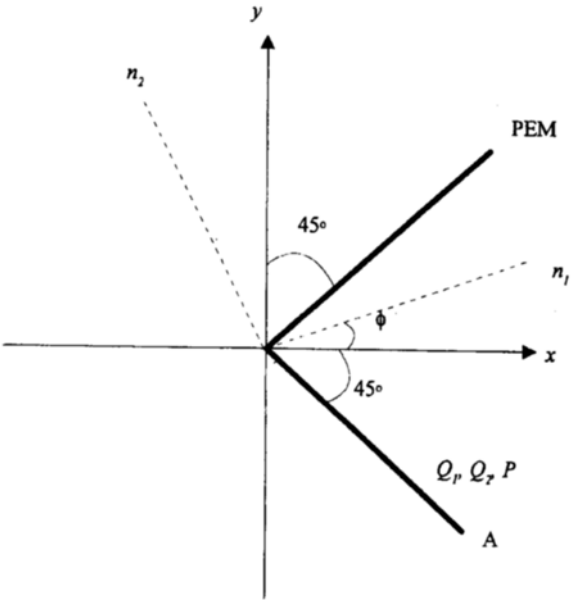

Fig. 2. Relative directions of optical elements.

A : Analyer
P : Polarizer
PEM : Photo-elastic modulator
Q1, Q2 : Upper and lower quarter-wave plates
n1, n2 : Major and minor values of refractive index tensor
ϕ : Orientation angle of sample

Total intensity I of the output light, the first element of the Stokes vector **S**, can be divided into terms related to mean, first and second harmonic intensities I_{dc}, I_ω, $I_{2\omega}$ to the reference fre-

quency ω of PEM through a Fourier series expansion.

$$I = I_{dc} + I_{\omega} \sin\omega t + I_{2\omega} \cos 2\omega t + \cdots \quad (5)$$

In the above equation, I_{dc}, I_{ω}, $I_{2\omega}$ are measured data. Birefringence Δn of the solution is given experimentally from the relation to the phase retardance δ.

$$\Delta n = \frac{\lambda\delta}{2\pi d}. \quad (6)$$

Here λ is the wavelength of He-Ne laser light, d is the sample depth, and phase retardance δ is given as follows ;

$$\delta = \sin^{-1}[(I_{\omega}/2I_{dc}J_1)^2 + (I_{2\omega}/2I_{dc}J_2)^2]^{1/2} \quad (7)$$

where J_1 and J_2 are the first and second Bessel functions determined by the calibration procedure of the given PMFB system. The extinction angle is also experimentally given by

$$\chi = \frac{1}{2}\tan^{-1}\left(\frac{I_{2\omega}/J_2}{I_{\omega}/J_1}\right). \quad (8)$$

2. Apparatus and Experimental Procedure

As shown in Fig. 1, the whole apparatus can be divided into three parts : the arranged optical components including the streaming Kerr cell, the instrumental part for applying the external fields on the cell, and the part controlling the whole system and processing data. In addition to the usual apparatus used in flow birefringence experiment, a streaming Kerr cell and an electric pulse generator are needed for the experiments under the combined fields.

Streaming Kerr Cell--Fig. 3 is the schematic diagram of the streaming Kerr cell used in this study. The basic design of the streaming Kerr cell is similar to the ordinary streaming flow cell with a double concentric Couette geometry. The outer cylinder is rotated to induce the simple shear flow (V_x=Gy), and the electric field, E_0, perpendicular to the flow direction is applied by an electric pulse generator. The light is sent through the gap between the inner cylinder and the rotating outer cylinder and finally detected at the photo-detector. In order to perform combined field experiments, the streaming Kerr cell has been carefully manufactured with following considerations. Dielectric breakdown is primarily determined by the dielectric property of the object solution, but it is also largely affected by the choice of material and surface conditions of the cell electrodes. In the case of using a duralumin cell, the usual copper or stainless steel electrodes will give dielectric breakdown at the electric field strengths of about 14-20 kV/cm so that deterioration of the solution would be serious. In order to restrain such dielectric breakdown and deterioration of the solution, the electrode surfaces of the cell were finely finished and coated by triple plating film of Ni-Gd-Pt. Electric insulation above MΩ and grounding treatment of electrodes were also considered.

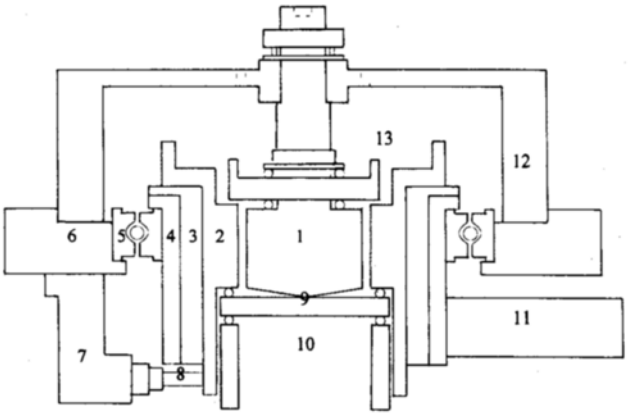

Fig. 3. Schematic diagram of the streaming Kerr cell.

1. Inner cylinder
2. Outer cylinder
3. Tefron insulator
4. Timing-belt pully
5. Bearing
6. Base
7. Electric brush holder
8. Electric carbon brush
9. Optic glass
10. Vite O-ring
11. Timing-belt
12. Inner cylinder cap
13. Baffle ring

Electric Pulse Generator--In general, it is difficult to apply a high electric field for a long time because of the bubble generation by polarization and Joule heating due to low internal resistance of cells. And the capacitance of solution would alter the shape of the electric pulse itself from that of the ideal pulse. In order to apply clear and exact electric fields on the cell containing the polymer solution, the electrical property of the cell should be considered in advance. A cell usually has both resistor and capacitance characteristics and these are closely related to the specification of an electric pulse generator. Thus, the electric pulse experiments are usually performed considering the characteristic time scale of molecules in solution. The electric pulse method has been widely used to study the dynamics of electric birefringence in colloidal systems and solutions of the virus, nucleic acid, protein, and many other biogenic materials [Fredricq and Houssier, 1973; Tricot and Houssier, 1982]. A high voltage pulse was loaded on the cell by a spark discharge. The pulse duration time was adjusted by the combination of RC element and Hg-wet magnet.

Other devices used in this study are a photo-elastic modulator for sine wave phase modulation, a compumotor for inception of shear flow field to the cell, a clutch/brake for switching of power transfer, two lock-in amplifiers with low pass filter function for filtering of output signal, a data storage oscilloscope for storage and processing of data and a computer for the control of whole experiments.

3. Materials

Object solutions suitable for the birefringence experiment have some basic restrictions : they must be optically transparent and the size of solute particles should be less than the wavelength of source light. Polymer solutions used in the present experiments are m-cresol (η_0=0.0128 Pa·s) with PBLG havng molecular weight of 4 sizes ranging from 15,000 to 236,000. PBLG polymers were purchased from Sigma Chemical Co., and no further purification was performed.

To investigate the effects of the interaction between polymers, two series of solutions of 0.03644 and 0.1 g/dL concentrations were selected. At the higher concentration, it can form a lyotropic state as shown elsewhere [Kim et al., 1995]. It is

Table 1. m-Cresol solution of poly(γ-benzyl-L-glutamate) used

Solution	Molecular weight	Concentration [g/dL]
I	236,000	0.1
II	236,000	0.03644
III	86,000	0.1
IV	86,000	0.03644
V	51,000	0.1
VI	15,000	0.1

well known that PBLG polymers dissolved in these solutions are somewhat rigid under this experimental condition and temperature range of about 23-25 °C. Specifications of PBLG/m-cresol solutions used in this experiment are summarized in Table 1.

RESULTS AND DISCUSSION

The electrohydrodynamic properties of PBLG/m-cresol solution are determined in terms of birefringence and extinction angle. The external fields are composed of both simple shear flow field (V_x=Gy) and uniform electric field, E_0, perpendicular to the shear direction in the x-y plane. The experimental results are compared with the theoretical prediction from previous works [Kwon and Park, 1992]. Consequently, parameters including D_r, $VB_d\mu_o$, C are obtained. To appreciate complicated responses of the solution due to the external fields, it is preferred to examine the transient behaviors in the first place.

1. Transient Birefringence Experiment

Fig. 4 represents the typical results of transient birefringence pattern under several strengths of shear flow. As shown in the figure, a shear flow field experiment with such a long pulse duration was proven to be an effective way to observe the inception, steady state, and relaxation flow characteristics, However, experimental difficulties such as clutch/brake time laps and mechanical vibration were also encountered.

Prior to applying the shear flow, the solution was allowed to stand at rest long enough to ensure the static equilibrium. As the shear flow strength increased, the birefringence increased while the time to reach the first peak took a little longer. In all the cases, distinct oscillatory behavior with a constant period of about 24 msec was observed after the flow inception. These oscillatory patterns are mainly due to the shear wave propagation following the inception of the simple shear flow.

Since PBLG polymers dissolved in m-cresol have a characteristic time scale τ_c of a few msec (for these experiments, τ_r(=1/6D_r) of PBLG polymers is 1.56 msec), their molecular dynamics is principally governed by such a time scale. In transient shear flow of Newtonian fluids, the momentum generated from the moving boundary is transferred to the interior of the fluid by means of the diffusive mechanism. The characteristic time τ_d to reach the steady state is known as follows [Lee and Fuller, 1991].

$$\tau_d=\frac{L^2}{\nu}, \tag{9}$$

where L is the measuring position (roughly equal to the half of the gap width of the cell) and ν is the kinematic viscosity of the solution. In our case, the viscosity of m-cresol is 12.8 cP at 25 °C and L is 0.615 mm, so that the characteristic time to reach the steady state, τ_d, would be approximately 31.0 msec. Considering the molecular characteristic time τ_c(=1.56 msec), it is certain that the change of the applied shear flow field is governed by the diffusive time scale of the flow.

The inception experiment under strong flow fields is restricted by the mechanical overload. A slight distortion seen during the rise of birefringence when G=90 sec^{-1} is due to the sudden

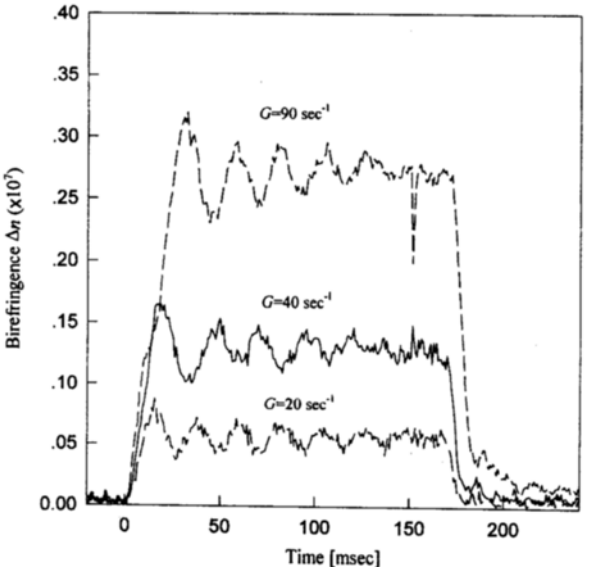

Fig. 4. Transient birefringence by rectangular shear flow field using 0.1 g/dL m-cresol solution (solution I) of PBLG with M.W.=236,000.

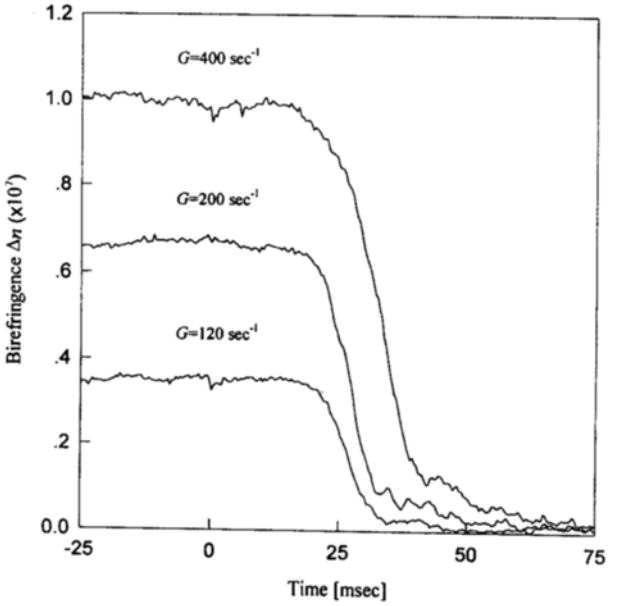

Fig. 5. Transient birefringence before and after cessation of high shear flow field applied to 0.1 g/dL m-cresol solution (solution I) of PBLG with M.W.=236,000.

application of a strong flow field. Flow birefringence under high strong fields (up to 400 sec^{-1} in our experiments) was measured by accelerating the Kerr cell keeping the clutch on. Fig. 5 represents the birefringence pattern after the strong flow field ceased (at t=0). As seen in this figure, birefringence still remained for about 20 msec even after the external shear flow field was removed. This implies that shear wave propagation is the dominant factor in this experiment. After 20 msec, birefringence relaxed back to the original value with an S-shaped pattern, resulting in a longer relaxation time for the stronger field. A peak near 150 msec when G is 90 sec^{-1} in Fig. 4 and small tips at t=0 sec in Fig. 5 are all due to a piezoelectric effect. Such a piezoelectricity, which resulted from the alignment of dipolar particles in the solution along the extinction angle, happened more frequently when the flow field was strong and long.

The electric field strength in a birefringence experiment is limited by a solution's electric properties. When the solution is exposed to its limiting electric field, its basic electric properties are usually altered in a destructive way. Therefore, in electric birefringence experiments, the pulsed type has been widely used. In this study, a squarely pulsed electric field was applied in order to estimate the electric birefringence. Fig. 6(a) shows the typical electric birefringence pattern as a function of electric field strength. The electric birefringence pattern shows a relatively clear shape with less noise compared to that obtained in flow birefringence experiments. In the region of a weak field, the birefringence exhibited a stable steady state. It appears that in this region the electric field is evenly balanced with the Brownian randomizing force of PBLG molecules. As the electric field became strong, the overshoot of birefringence was observed and the time to reach the steady state increased.

Fig. 6(b) is a typical example of the extinction angle obtained from a transient electric birefringence experiment when E_0 is 19.4 kV/cm. As shown in the figure, scattered traces of the extinction angle before and after the electric field is applied describe well the randomly isotropic state of the solution due to the Brownian motion of PBLG particles. Once the electric field is applied, the extinction angle immediately reaches 90° irrespective of the field strength.

Meanwhile, when no field is applied to the solution by disconnection of the electric field, then birefringence comes to depend solely on the particle's hydrodynamic property. Thus D_r of PBLG may be estimated directly. It is well known that D_r can be estimated from the slope of the semi-log plot between normalized birefringence and time in the relaxation region after the disconnection of the electric field. In the case of a monodispersed system, the relaxation birefringence can be represented as follows :

$$-\mathrm{Ln}(\Delta n/\Delta n_{|E\text{-field off}}) = 6D_r t. \quad (10)$$

Fig. 7 represents the semi-log plot of relaxation birefringence of three PBLG solutions with varying degree of molecular weight. In all cases, the linear relaxation birefringence indicates all solutions are uniformly dispersed. For solutions III and VI, disturbances after 2.7 and 3.2 msec, respectively, result from the limitation of our PMFB system's resolution. D_r value

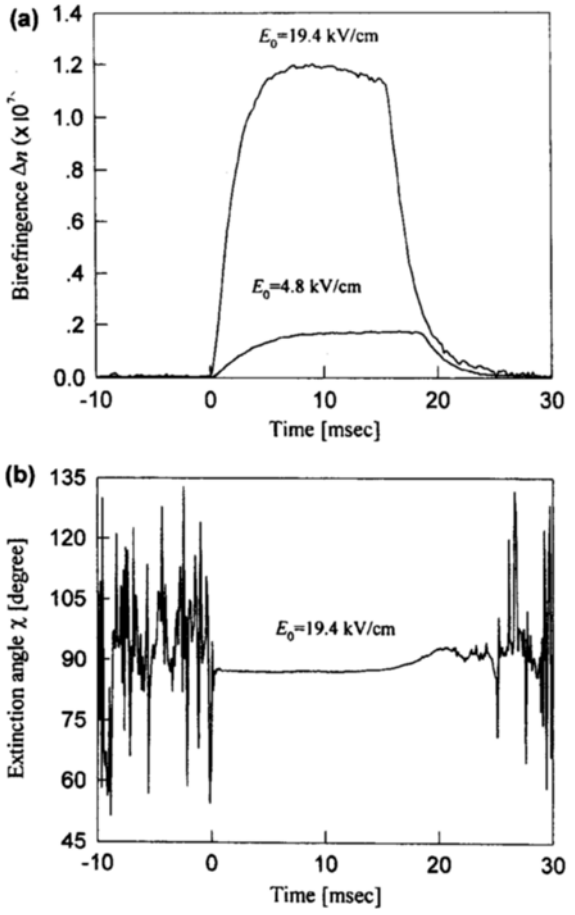

Fig. 6. Transient (a) birefringence Δn and (b) extinction angle χ by different pulsed electric fields using 0.1 g/dL m-cresol solution (solution I) of PBLG with M.W.= 236,000.

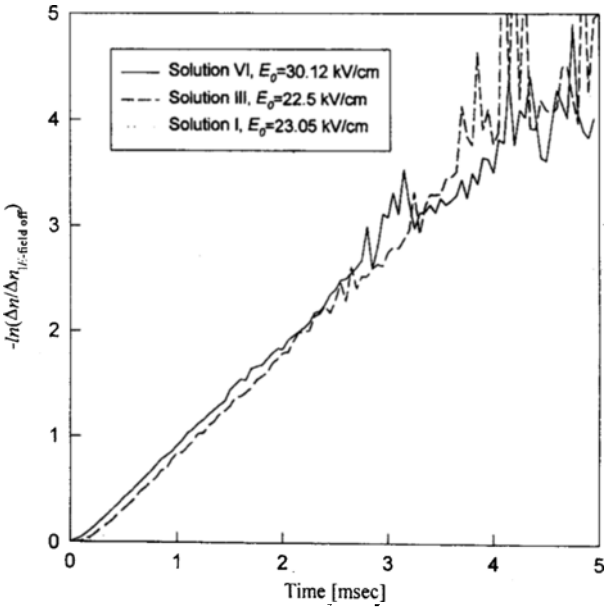

Fig. 7. Semi-logarithmic plot of normalized birefringence Δn/$\Delta n_{|E\text{-field off}}$ vs. time, in which $\Delta n_{|E\text{-field off}}$ is birefringence at the time when the electric field is off.

for solutions III and VI was estimated as 140 sec^{-1} and D_r for solution I was 65 sec^{-1} respectively. These values, however, are way off from the ratio of D_r values for solutions I, III and VI, 1 : 16 : 1740, estimated from Eq. (1) with the assumption that the length of the PBLG particles is proportional to the molecular weight. Such a large difference in D_r between the two results from the fact that the time constant (equal to 1 msec) of the low pass filter used in the lock-in amplifier is the same order or too large compared to the molecular time constant, τ_c, of PBLG. Accordingly, it turned out to be difficult to estimate D_r value under a transient electric field. Thus, the steady state experimental data were used to estimate D_r, as shown in the next section.

Fig. 8 represents the transient birefringence pattern under the combined field. Here a shear flow was introduced about 100 msec earlier before the electric field was imposed at t=0 and sustained for 10 msec. As shown in Fig. 8(a), the birefringence under the combined field is approximately 2.5 times larger than the value under the shear flow field only. It is yet difficult to estimate their respective contributions to the birefringence in the dimensionless value term. A clutch/brake

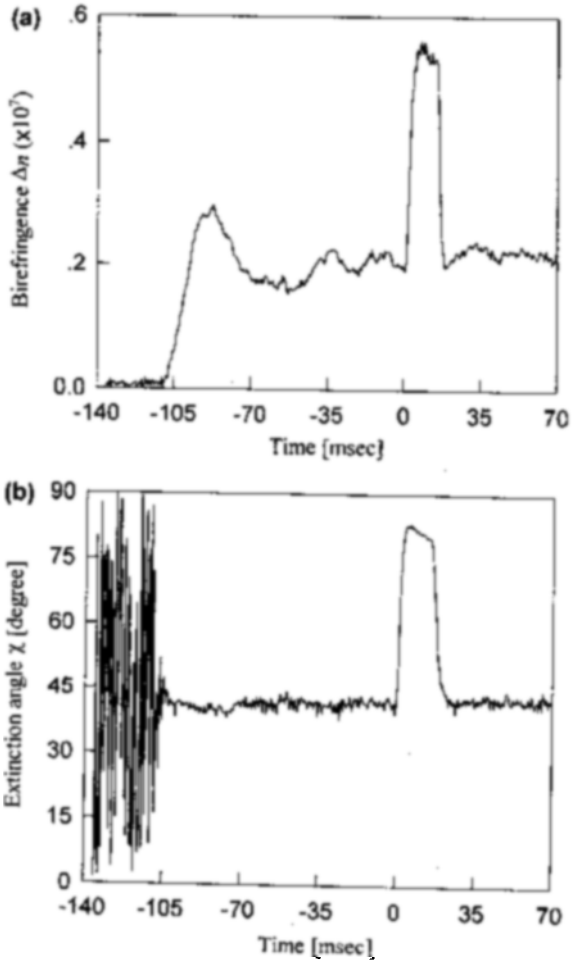

Fig. 8. Time dependence of (a) birefringence Δn and (b) extinction angle χ of 0.1 g/dL m-cresol solution of PBLG with M.W.=236,000, effected by pulsed electric field (E_0= 4.79 kV/cm) during the shear flow (G=60 sec^{-1}).

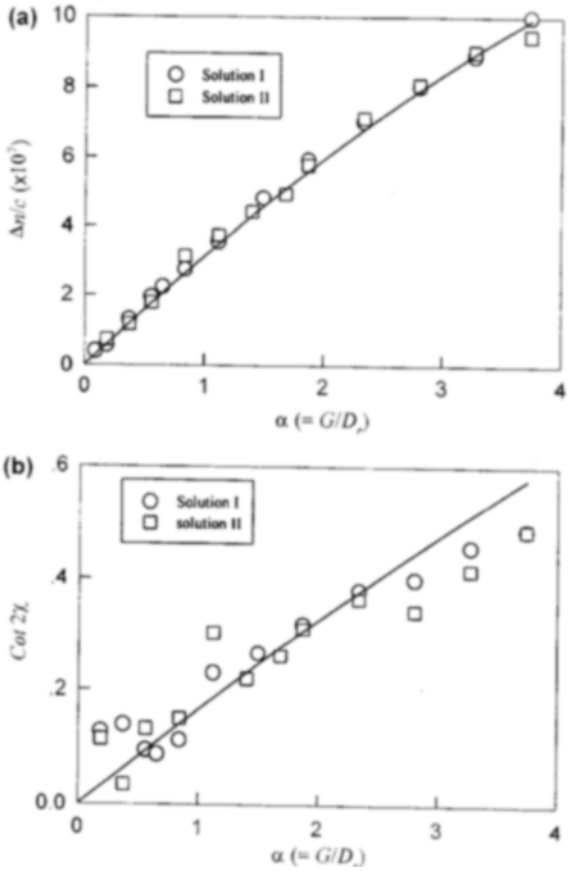

Fig. 9. Steady state electric birefringence of m-cresol solution of PBLG with M.W.=236,000. Solid line is the theoretical curve calculated using permanent dipole strength $VB_a\mu_0$=2,322 D and optical constant C=1.185×10^{-6}g/dL.

used in this experiment had mechanical delay time of about 30-200 msec, which made it difficult to extract the desired data in the memory range of a data storage oscilloscope. The combined field experiments were carefully scheduled to contain the desired data and have a good resolution of data. And the experiments involving a strong shear field were designed such that relaxation region should be contained.

2. Steady State Results

Fig. 9(a) shows the birefringence results under steady shear flow field for two solutions with equal molecular weight, but with different concentration. As shown, the two results coincide with each other over the entire region. Moreover, a good correlation with the theoretical prediction is found. Since solutions I and II contain the largest molecular weight PBLG among the samples tested in this study, it is safe to say that all the solutions used are dilute ones. Slight scattering in the extinction angle data in Fig. 9(b) indicates that the extinction angle is sensitive in weak flow fields. Electric birefringence was measured in order to investigate whether the solution is electrically dilute or not.

Fig. 10 shows the birefringence results obtained from a series of electric field experiments, compared with the theoretical prediction. Birefringence data agree well with each other up to E_0 equal to about 18 kV/cm, irrespective of both molecular weight

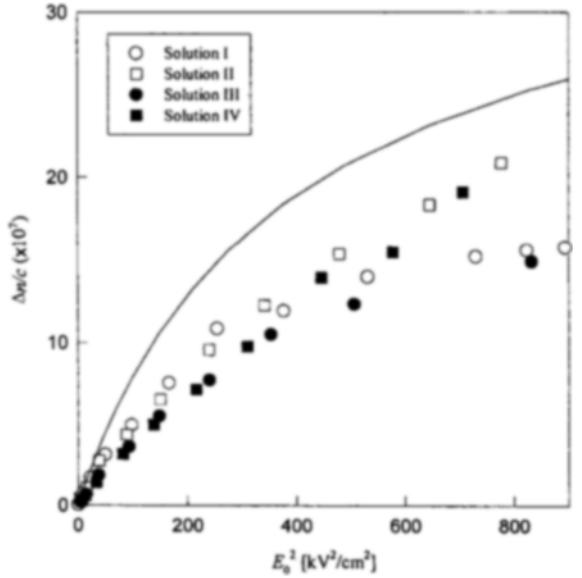

Fig. 10. Steady state birefringence vs. square of electric field strength E_0^2 for m-cresol solutions of PBLG with M.W.= 236,000 and 86,000, respectively. Solid line is the theoretical curve calculated using rotational diffusivity D_r= 80.355 sec^{-1} and optical constant C=1.185×10^{-6} g/dL.

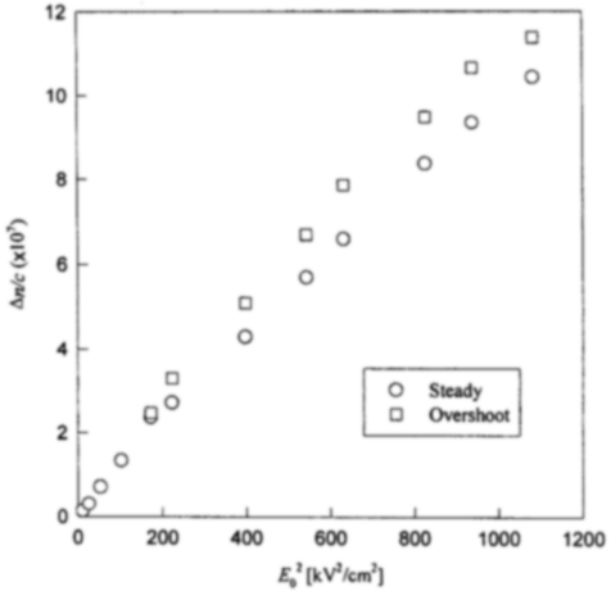

Fig. 11. Steady and overshoot birefringence vs. square of electric field strength E_0^2 on 0.1 g/dL m-cresol solutions of PBLG with M.W.=51,000.

and concentration. As the electric field becomes stronger, the birefringence of concentrated solutions I and III increases more slowly than dilute solutions II and IV due to the electric hindrance. We can say that the electric field strength for the electric hindrance to appear depends mainly on the weight concentration.

As the electric field duration is longer, the overshoot pattern is seen on the birefringence trace of PBLG solutions under strong fields. Such a tendency becomes more conspicuous with PBLG of low molecular weights. Figs. 11 and 12

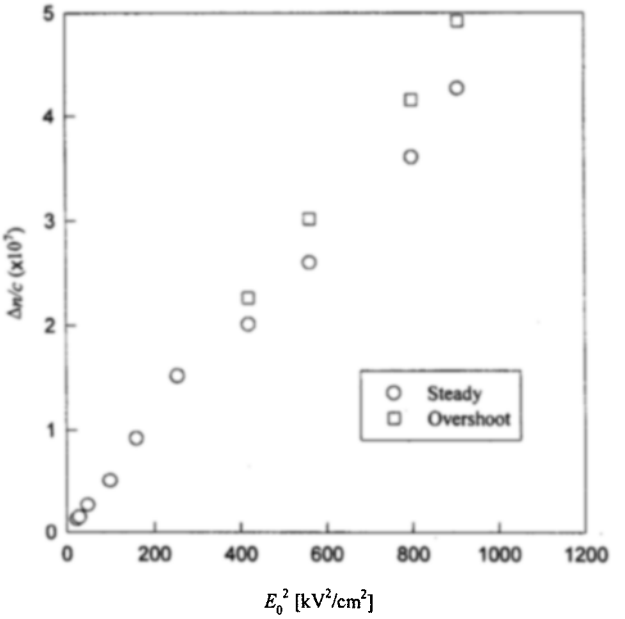

Fig. 12. Steady and overshoot birefringence vs. square of electric field strength E_0^2 on 0.1 g/dL m-cresol solutions of PBLG with M.W.=15,000.

represent the birefringence obtained from electric field experiments with relatively long pulse duration using solution V (M.W. equal to 51,000) and VI (M.W. equal to 15,000) in Table 1. Overshoot was observed above a certain electric field strength, and increased as the field strength increases. The ratio of overshoot to steady state had larger values in the case of low molecular weight PBLG. Although successive application of an electric field made the birefringence value decrease slowly due to the deterioration of solution, the overshoot ratio did not change. Therefore, it can be said that the overshoot is discriminated from the deterioration of the solution.

Fig. 13 represents the typical results under combined fields. The stronger the field is, the more difficult it was to fit the theoretical prediction with the experimental values. Therefore, weak field data were mainly used to perform the parameter fitting while strong field data were considered for reference. In the case of α equal to 0.56, although it had a strong electric field, relatively close fitting between the theoretical and experimental data was found. This is believed to be due to the fact that the extinction angle reaches a limiting value. Consequently, through numerous comparisons, D_r equal to 107 sec^{-1}, VB_a μ_0 2,300 Debye, and C 1.58×10^{-6} were estimated. The calculations in this study were all based on these values.

Two things should be checked if the combined field experiments are to be interpreted. In the first, it is the capacity of the electric pulse generator, PG, in relation to the object solution. When the electrical resistance of the test solution is considerably low, it may cause the dielectric relaxation of PG itself. In addition, it is imperative to check if there is any voltage drop, overshoot or sag of PG, and how fast the pulse rise compared with τ_c of PBLG is. It is also important to check whether the desired voltage is properly applied under the combined fields.

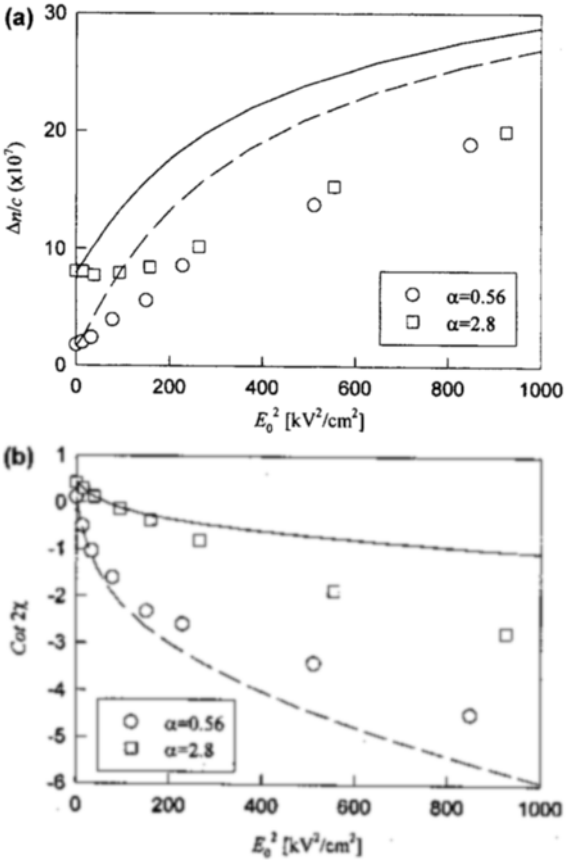

Fig. 13. Steady state (a) birefringence and (b) cot2χ of solution II under combined fields vs. square of electric field strength E_0^2. Theoretical curves were calculated using D_r=107 sec^{-1}, $VB_a\mu_0$=2,322 D and optical constant C=1.185×10^{-6} g/dL in which solid lines are for α=2.8 and dashed lines for α=0.56.

CONCLUSION

Birefringence experiments were performed to investigate the optical state of dilute m-cresol solutions of poly(γ-benzyl-L-glutamate), PBLG, having molecular weights of 4 sizes ranging from 15,000 to 236,000. Under the combined fields (composed of shear flow and electric fields) in the wide range of field strength in which maximum shear rate was 400 sec^{-1} and electric field was loaded up to 33 kV/cm, transient birefringence and extinction angle were simultaneously measured by using the phase-modulated birefringence method. Respective intrinsic characteristics of the component and the combined fields were discussed through the representative transient experiments. Steady state results from the combined fields were compared with the theoretical prediction through simultaneous multiple parameters fitting. In experiments using PBLG solutions with its molecular weight of 236,000, the rotational diffusivity of a PBLG molecule, D_r, was estimated at 107 sec^{-1}, permanent dipole strength, $VB_a\mu_0$, 2,300 Debye unit, and optical constant of the solution, C, 1.58×10^{-6}. The optical state of a solution being tested could be, to a certain extent, explained by the dimensionless field parameters established in the previous theory. However, mainly due to electric hindrance, flow instability by the strongly combined fields, deterioration of a solution by successive electric field experiments, etc., the experimental values showed some deviations from the theoretical values. In experiments to investigate the concentration dependence on the interaction effects between PBLG molecules, the hydrodynamic interactions were not noticed within a experimented range, but electric effects were sensitive to both the applied electric field strength and the concentration of the solution.

NOMENCLATURE

a, b : half lengths of a polymer molecule in major and minor axes
B_a : internal field function
C : optical constant of solution
d : sample depth
D : Debye unit
D_r : rotational diffusivity of a polymer molecule
E_0 : electric field strength applied
G : shear rate
I : total intensity of output light, the first element of Stokes vector **S**
I_{dc}, I_w, I_{2w} : mean, first and second harmonic intensities of total intensity I
J_1, J_2 : first and second Bessel functions
k : Boltzmann constant
L : measuring position length
$\mathbf{M}_i$: Muller matrix of each optical component i
r : aspect ratio of major and minor axis, given by a/b
$r^2Q(r)$: geometric factor of a polymer molecule
S : Stokes vector
$\mathbf{S}_0$: Stokes vector of input light
t : time
T : absolute temperature
V : volume of a particle molecule
V_x : velocity in x-axis direction
x, y : coordinates

Greek Letters

α : Peclet number
β : dimensionless parameter related to the permanent dipole moment of a polymer molecule
δ : phase retardance
Δn : birefringence
η_0 : solvent viscosity
λ : wavelength of He-Ne laser light
μ_0 : permanent dipole moment per unit volume of a polymer molecule
ν : kinematic viscosity
τ_d : characteristic time of fluid by diffusive mechanism
τ_c : characteristic time of a polymer molecule
χ : extinction angle of polymer solution
ω : reference frequency of photo-elastic modulator

REFERENCES

Arp, P. A., Foister, R. T. and Mason, S. G., "Some Electrohydro-

dynamic Effects in Fluid Dispersions," *Adv. Colloid Interface Sci.*, **12**, 295 (1980).

Frattini, P. L. and Fuller, G. G., "A Note on Phase-Modulated Flow Birefringence : A Promising Rheo-Optical Method," *J. Rheol.*, **28**, 61 (1984).

Fredericq, E. and Houssier, C., "Electric Dichroism and Electric Birefringence," Clarendon Press, Oxford (1973).

Hwang, C. I., Lim, T. J. and Park, O. O., "Computer-Aided Phase Modulated Flow Birefringence Experiment on Polystyrene Solution," *Korean J. Chem. Eng.*, **6**, 23 (1989).

Ikeda, S., "Orientation Birefringence of Macromolecular Solutions in Shear Flow and Electric Field," *J. Chem. Phys.*, **38**, 2839 (1963).

Kim, D. H., Kim, K. M. and Park, O. O., "Structural Oscillation of the Poly(g-benzyl-L-glutamate) Solution after Reversal of Shear Flow," *Nihon Reoroji Gakkaishi*, **23**, 39 (1995).

Kwon, M. H. and Park, O. O., "Electrohydrodynamics of Rigid Macromolecules with Permanent and Induced Dipole Moments. II," *J. Rheol.*, **36**, 507 (1992).

Lee, J. S. and Fuller, G. G., "Shear Wave Propagation after Stepwise Increase of Shear Rate," *J. Non-Newtonian Fluid Mech.*, **39**, 1 (1991).

Meeten, G. H., "Optical Properties of Polymers," Elsevier App. Sci. Pub., London and New York (1986).

Mukohata, Y., Ikeda, S. and Isemura, T., "The Electric-Streaming Birefringence of Poly(γ-benzyl-L-glutamate) in m-Cresol," *J. Mol. Biol.*, **5**, 570 (1962).

Oh, Y. R. and. Park, O. O., "Transient Flow Birefringence of Calf Skin Collagen Solutions," *J. Chem. Eng. Japan*, **25**, 243 (1992).

O'Konski, C. T., Yoshioka, K. and Orttung, W. H., "Electric Properties of Macromolecules. IV. Determination of Electric and Optical Parameters from Saturation of Electric Birefringence in Solutions," *J. Phys. Chem.*, **63**, 1558 (1959).

O'Konski, C. T., K.(ed.), "Molecular Electro-Optics," part 1 & 2, Marcel Dekker, Inc., New York (1976).

Park, O. O., "Electrohydrodynamics of Rigid Macromolecules with Permanent and Induced Dipole Moments," *J. Rheol.*, **32**, 511 (1988).

Park, O. O., "Flexible and Rigid Macromolecule in Shear and Electric Fields," *Korean J. Chem. Eng.*, **6**, 282 (1989).

Shurcliff, W. A., "Polarized Light : Production and Use," Harvard Univ. Press (1962).

Tricot, M. and Houssier, C., "Electrooptical Studies on Sodium Poly(styrenesulfonate). 1. Electric Polarizability and Orientation Function from Electric Birefringence Measurements," *Macromolec-ules*, **15**, 854 (1982).

Wada, A., "Dielectric Properties of Polypeptide Solutions. II. Relation between the Electric Dipole Moment and the Molecular Weight of a α Helix," *J. Chem. Phys.*, **30**, 328 (1959).